Ag-doped ZnO nanorods synthesized by two-step method*

Chen Xian-Mei(陈先梅), Ji Yong(冀 勇), Gao Xiao-Yong(郜小勇)†, and Zhao Xian-Wei(赵显伟)

Key Laboratory of Material Physics of Ministry of Education, School of Physics and Engineering, Zhengzhou University, Zhengzhou 450052, *China*

(Received 22 March 2012; revised manuscript received 26 April 2012)

A two-step method is adopted to synthesize Ag-doped ZnO nanorods. A ZnO seed layer is first prepared on a glass substrate by thermal decomposition of zinc acetate. Ag-doped ZnO nanorods are then assembled on the ZnO seed layer using the hydrothermal method. The influences of the molar percentage of Ag ions to Zn ions ($R_{\mathrm{Ag/Zn}}$) on the structural and optical properties of the ZnO nanorods obtained are carefully studied using X-ray diffractometry, scanning electron microscopy and spectrophotometry. Results indicate that Ag ions enter into the crystal lattice through the substitution of Zn ions. The $\langle 002 \rangle$ c-axis-preferred orientation of the ZnO nanorods decreases as $R_{\mathrm{Ag/Zn}}$ increases. At $R_{\mathrm{Ag/Zn}} > 1.0\%$, ZnO nanorods lose their c-axis-preferred orientation and generate Ag precipitates from the ZnO crystal lattice. The average transmissivity in the visible region first increases and then decreases as $R_{\mathrm{Ag/Zn}}$ increases. The absorption edge is first blue shifted and then red shifted. The influence of Ag doping on the average head face, and axial dimensions of the ZnO nanorods may be optimized to improve the average transmissivity at $R_{\mathrm{Ag/Zn}} < 1.0\%$.

Keywords: ZnO nanorods, Ag doping, thermal decomposition of zinc acetate, hydrothermal method

PACS: 68.35.bj, 81.10.–h, 91.60.Ed, 91.60.Mk **DOI:** 10.1088/1674-1056/21/11/116801

1. Introduction

Zinc oxide (ZnO) is a semiconductor with a wide band gap (3.37 eV) and a large binding energy (60 meV).[1] As ZnO has exceptional electronic and optical properties, it has been widely studied for high-technology applications, including a variety of UV and blue/blue-green light-emitting diodes, solar cells, piezoelectric transducers, surface acoustic wave devices, gas sensors, displays and lighting.[2,3] Several techniques have been proposed to prepare doped ZnO, including the sol-gel method,[4] metal organic chemical vapor deposition,[5] spray pyrolysis,[6] RF magnetron sputtering,[7] DC magnetron sputtering,[8] medium-frequency magnetron sputtering,[9] pulsed laser deposition,[10] etc. Unfortunately, these techniques require harsh reaction conditions, entail high costs, and have low selectivity to impurities. In contrast, hydrothermal preparation of ZnO on ZnO seed layer by thermal decomposition of zinc acetate features lower costs, a simple process, and use of easily accessible raw materials. Moreover, the hydrothermal method can easily be controlled and is highly selective to impurities. These advantages make the method ideal for producing ZnO nanorods. However, while the method is reported,[11] studies on the preparation of Ag-doped ZnO nanorods using the hydrothermal method have not yet been published. The hydrothermal method involves a series of processes, including dissolution, generated mixture, hydrolysis, polymerization, and crystallization. After $Zn(CH_3COO)_2{\cdot}2H_2O$ is dissolved in ethanol solution, the compound breaks down to generate the ZnO seed layer under heating conditions, as shown below[12−14]

$$\mathrm{Zn(CH_3COO)_2 \cdot 2H_2O} \rightarrow \mathrm{2CH_3COOH\uparrow + ZnO + 2H_2O\uparrow}.$$

A two-step method is used in this study. The ZnO seed layer is first prepared on a glass substrate by thermal decomposition of zinc acetate. Ag-doped ZnO nanorods are then assembled on the ZnO seed layer using the hydrothermal method. We discuss the influences of the molar percentage of Ag ions to Zn ions ($R_{\mathrm{Ag/Zn}}$) on the structure of the ZnO nanorods, their absorption, and, more importantly, the average

*Projected supported by the National Natural Science Foundation of China (Grant No. 60807001), the Foundation of Henan Educational Committee, China (Grant No. 2010A140017), the Henan Provincial College Young Teachers Program, China, and the Graduate Innovation of Zhengzhou University, China (Grant No. 11L10102).

†Corresponding author. E-mail: xygao@zzu.edu.cn

© 2012 Chinese Physical Society and IOP Publishing Ltd

transmissivity. The results obtained are expected to be able to contribute to the future applications of ZnO in solar cell electrodes.

2. Experimental procedure

A glass substrate was rinsed sequentially with acetone, alcohol, and deionized water in an ultrasonic bath for 10 min to remove grease, soluble organic compounds, and other contaminants that could affect the quality of the ZnO nanorods from its surface. Ag-doped ZnO nanorods were then synthesized using an ethanol solution of zinc acetate (0.02 mol/L), silver nitrate solution (0.002 mol/L), zinc nitrate aqueous solution (0.025 mol/L), and hexamethylenetetramine solution (0.025 mol/L). As direct deposition of ZnO film on the glass substrate by the hydrothermal method is difficult to achieve, we prepared a seed layer on the surface of the glass substrate to improve its adsorption property.

A ZnO seed layer was prepared on the glass substrate by thermal decomposition of zinc acetate. The glass substrate was immersed in an ethanol solution of zinc acetate for 10 s or so and then dried using a hair dryer; this process was repeated seven to nine times. The glass substrate was heated to 350 °C for 20 min in air, and the zinc acetate decomposed into the ZnO seed layer. About 20 mL of zinc nitrate solution and 20 mL of hexamethylenetetramine solution were subsequently added into each autoclave, followed by the addition of different volumes (i.e., 0 mL, 2 mL, 2.25 mL, 2.5 mL, and 3 mL corresponding to $R_{\mathrm{Ag/Zn}}$ of 0.0%, 0.8%, 0.9%, 1.0%, and 1.2%, respectively) of silver nitrate solution. The ZnO seed layer was then placed in the mixed aqueous solution vertically at 95 °C for 6 h. Thereafter, the sample was washed several times with deionized water until adsorbed ions were removed from the surface. Finally, the sample was dried in an oven at 60 °C for 24 h.

The structure of the doped ZnO nanorods was determined by X-ray diffraction (XRD). The surface microstructure was obtained by a cold field scanning electron microscope (SEM) (JEOL-JSM-6700 F) operating at a voltage of 10 keV. Optical properties were measured through spectrophotometry (Shimadzu UV-3150).

3. Results and discussion

Figure 1 shows SEM images of the ZnO nanorods at different values of $R_{\mathrm{Ag/Zn}}$ and Table 1 presents the average head face and axial dimensions of the ZnO nanorods obtained based on the SEM images.

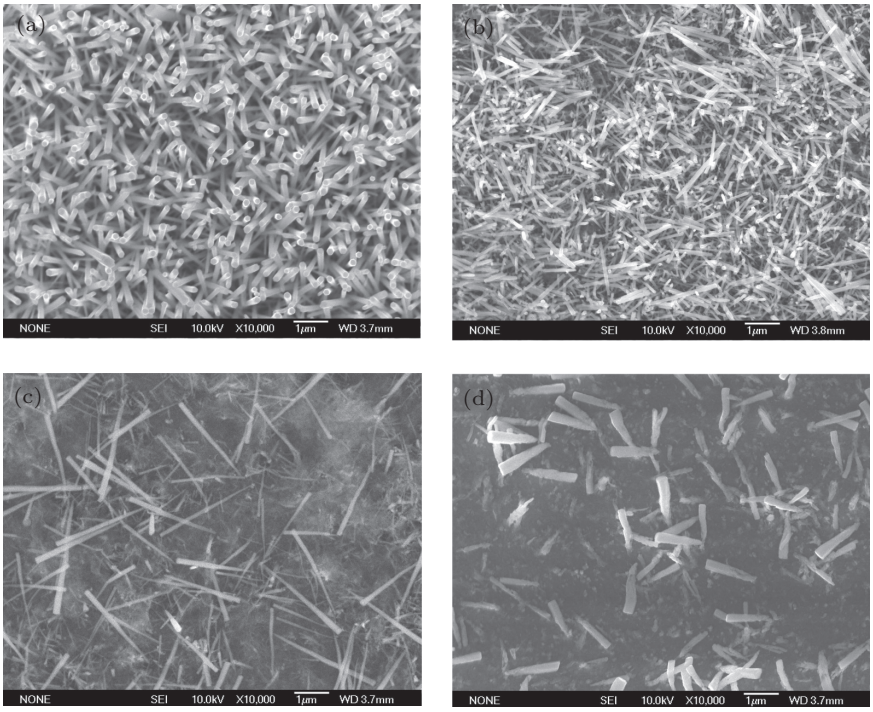


Fig. 1. SEM images of the ZnO nanorods at $R_{\mathrm{Ag/Zn}}$ of (a) 0%, (b) 0.8%, (c) 1.0%, (d) 1.2%, respectively.

Figure 1 and Table 1 demonstrate that undoped ZnO nanorods grow in the direction perpendicular to the substrate. Compared with undoped ZnO nanorods, Ag-doped ZnO nanorods are thin and short. With the value of $R_{\mathrm{Ag/Zn}}$ increasing, the angle by which ZnO nanorods deviate vertically from the substrate becomes larger and the lattice hexagonal structure of ZnO nanorods is reduced; the $\langle 002 \rangle$ c-axis-preferred orientation is eventually lost, as shown in Fig. 2.

Table 1. Average head face and axial dimensions of the ZnO nanorods at different values of $R_{\mathrm{Ag/Zn}}$.

$R_{\mathrm{Ag/Zn}}$/%	Average head face dimension/nm	Average axial dimension/nm
0.0	200	2700
0.8	97	1967
0.9	90	2467
1.0	125	2633
1.2	325	1500

Figure 2 shows the XRD patterns of the ZnO nanorods obtained at different values of $R_{\mathrm{Ag/Zn}}$. The ZnO nanorods are of a hexagonal polycrystalline structure, featuring a sharp and strong ZnO (002) diffraction peak and several other weak ZnO (100), (101), (102), (103), and (201) diffraction peaks. Clearly, the ZnO nanorods have (002) c-axis-preferred orientation at $R_{\mathrm{Ag/Zn}} \leq 0.9\%$. The c-axis-preferred orientation of ZnO nanorods is reduced significantly, and even lost, as the value of $R_{\mathrm{Ag/Zn}}$ increases. In addition, the ZnO (100), (101), (102), (103), and (201) diffraction peaks indicate that the orientation of the ZnO nanorods is random. Compared with the case of undoped ZnO, the 2θ of the ZnO (002) diffraction peak of Ag-doped ZnO nanorods decreases as the value of $R_{\mathrm{Ag/Zn}}$ increases. This phenomenon is caused by Ag ions entering the crystal lattice through the substitution of Zn ions, causing the variable length of the ZnO c axis. The variable length of the c axis indicates that the ZnO nanorods mainly experience compressive stress and further proves that Ag has been successfully doped into the ZnO lattice. The intensity of the diffraction peaks and the crystallization of the ZnO nanorods decrease with the increasing value of $R_{\mathrm{Ag/Zn}}$. These results can be attributed to the adverse effects of the stress on Ag-doped ZnO nanorods.[15] Figure 2 shows the Ag (111) diffraction peak at $R_{\mathrm{Ag/Zn}} \geq 1.0\%$. With the value of $R_{\mathrm{Ag/Zn}}$ increasing, the intensity of the Ag (111) diffraction peak increases. Such a change may be attributed to the maximum dissolution of Ag ions in the ZnO lattice, achieved at $R_{\mathrm{Ag/Zn}} = 1.0\%$. At this value of $R_{\mathrm{Ag/Zn}}$, Ag is separated from the ZnO lattice and precipitates out.[14]

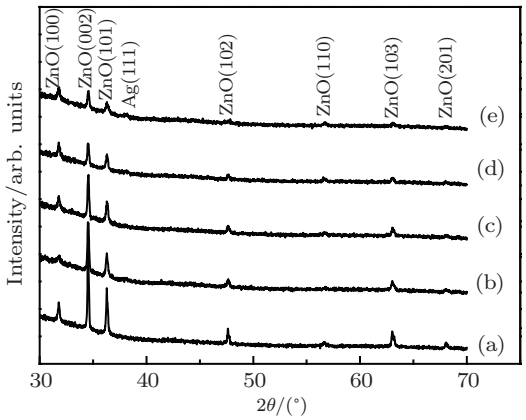


Fig. 2. X-ray diffraction patterns of the ZnO nanorods at $R_{\mathrm{Ag/Zn}}$ of (a) 0.0%, (b) 0.8%, (c) 0.9%, (d) 1.0%, (e) 1.2%, respectively.

Figures 3 and 4 respectively illustrate the transmissivity and absorption spectra of the ZnO nanorods at different values of $R_{\mathrm{Ag/Zn}}$. Both figures indicate that the absorption edge of ZnO nanorods at about 3.2 eV initially is blue shifted as the value of $R_{\mathrm{Ag/Zn}}$ increases and then red shifted at $R_{\mathrm{Ag/Zn}} > 1.0\%$. Figure 5 shows the average transmissivity of ZnO nanorods in the visible region. Figures 3 and 5 indicate that the transmissivity and average transmissivity of ZnO nanorods prepared through the hydrothermal method are lower in the visible region than those of ZnO thin films prepared by magnetron sputtering. Such low values may be caused by the poor qualities of the crystalline ZnO seed layer prepared through thermal decomposition of zinc acetate and the ZnO nanorods prepared through the hydrothermal method. In addition, figure 5 shows that the average transmissivity of Ag-doped ZnO nanorods is greater than that of undoped ZnO nanorods, which may be a result of the variable length of the c axis featured by Ag-doped ZnO nanorods. Table 1 indicates that the variation of transmissivity with the value of $R_{\mathrm{Ag/Zn}}$ is related to the average head face and axial dimensions of the ZnO nanorods. With the value of $R_{\mathrm{Ag/Zn}}$ increasing, the average transmissivity of the ZnO nanorods first increases fast and reaches a maximum at $R_{\mathrm{Ag/Zn}} = 0.9\%$, then decreases slowly. This phenomenon may be caused by common reductions in the average head face and axial dimensions

of the ZnO nanorods. The influence of Ag doping on the average head face and axial dimensions of the ZnO nanorods may be a dominant mechanism that can improve the average transmissivity of the ZnO nanorods. The improvement on average transmissivity is inherently attributed to the reduction of surface scattering closely related to the head face and axial dimensions. However, ZnO nanorods lose their *c*-axis-preferred orientation and Ag is separated out from the ZnO lattice at $R_{\mathrm{Ag/Zn}} > 1.0\%$, which may also result in the decrease in the average transmissivity and the enhancement in surface scattering related to head face and axial dimensions.

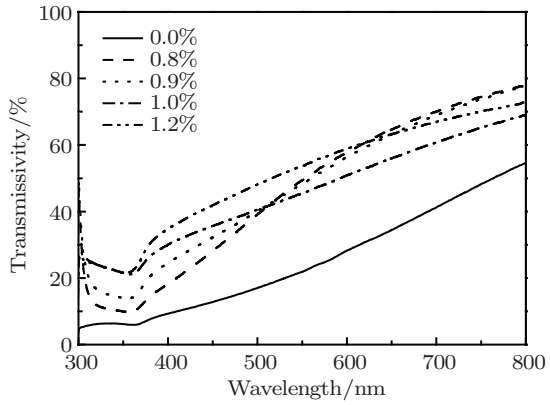


Fig. 3. Transmissivity spectra of the ZnO nanorods at different values of $R_{\mathrm{Ag/Zn}}$.

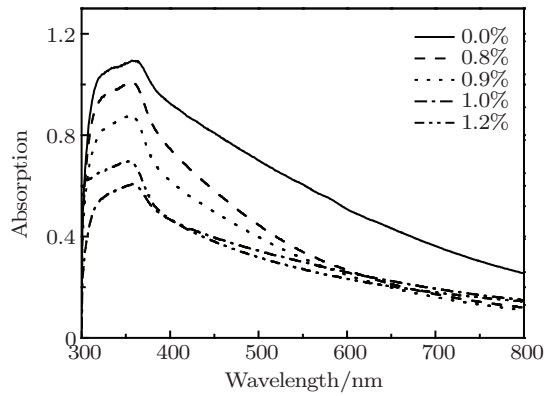


Fig. 4. Absorption spectra of the ZnO nanorods at different values of $R_{\mathrm{Ag/Zn}}$.

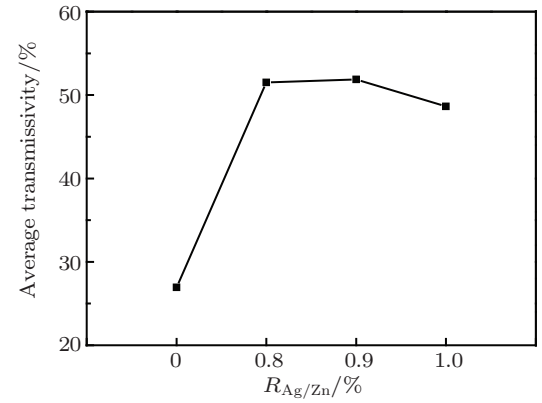


Fig. 5. Variation of the average transmissivity of ZnO nanorods in the visible region with the value of $R_{\mathrm{Ag/Zn}}$.

4. Conclusion

Ag-doped ZnO nanorods are successfully synthesized using the two-step method. The influences of $R_{\mathrm{Ag/Zn}}$ on the structural and optical properties of the ZnO nanorods are carefully studied. The main conclusions are listed as follows.

(1) The *c*-axis-preferred orientation of ZnO nanorods at $R_{\mathrm{Ag/Zn}} < 1.0\%$ is reduced, and even lost, as the value of $R_{\mathrm{Ag/Zn}}$ increases.

(2) The average transmissivity of the ZnO nanorods first increases fast and reaches a maximum at $R_{\mathrm{Ag/Zn}} = 0.9\%$, then decreases slowly with the value of $R_{\mathrm{Ag/Zn}}$ increasing. The increase in average transmissivity is caused by the influence of Ag doping on the average head face and axial dimensions of the ZnO nanorods. The improvement on the average transmissivity is inherently attributed to the reduction of surface scattering closely related to the head face and axial dimensions. The decrease in the average transmissivity is also attributed to the loss of *c*-axis-preferred orientation and Ag precipitation from the ZnO lattice and to the enhancement in surface scattering at $R_{\mathrm{Ag/Zn}} > 1.0\%$.

(3) Ag ions enter into the crystal lattice through the substitution of Zn ions, resulting in changes in the orientation, average head face, and axial dimensions of ZnO nanorods.

References

[1] Wang Y, Xu X L, Xie W Y, Wang Z B, Liu L and Zhao Y L 2008 *Acta Phys. Sin.* **57** 2582 (in Chinese)

[2] Yu J X, Huang B B, Qin X Y, Zhang X Y, Wang Z Y and Liu H X 2011 *Appl. Surf. Sci.* **257** 5563

[3] Zhao S Q, Yang L M, Liu W W, Zhao K, Zhou Y L and Zhou Q L 2010 *Chin. Phys.* B **19** 087204

[4] Li S S, Zhang Z, Huang J Z, Feng X P and Liu R X 2011 *Chin. Phys.* B **20** 127102

[5] Liu C H, Liu B C and Fu Z X 2008 *Chin. Phys.* B **17** 2292

[6] Seeber W T, Abou-Helal M O, Barth S, Beil D, Hoche T, Afify H H and Demian S E 1999 *Mat. Sci. Semicon. Proc.* **2** 45

[7] Peng L P, Fang L, Wu W D, Wang X M and Li L 2012 *Chin. Phys.* B **21** 047305

[8] Chen C, Ji Y, Gao X Y, Zhao M K, Ma J M, Zhang Z Y and Lu J X 2012 *Acta Phys. Sin.* **61** 036104 (in Chinese)

[9] Hong R J, Jiang X, Heide G, Szyszka B, Sittinger V, Xu S H, Werner W and Heide G 2003 *J. Cryst. Growth* **249** 461

[10] Wei X Q, Man B Y, Liu M, Xue C S, Zhuang H Z and Yang C 2007 *Physica* B **388** 145

[11] Ueno N, Maruo T, Norikazu N, Egashira Y and Ueyama K 2010 *Mater. Lett.* **64** 513

[12] Tang D X and Zhao Y 2003 *Chin. J. Chem. Phys.* **16** 237 (in Chinese)

[13] Zhao X Y, Li C Z, Zheng B C, Gu H C and Hu LM 1997 *Journal of East China University of Science and Technology* **23** 191 (in Chinese)

[14] Lu M M, Ma X M and Cheng W J 2009 *J. Synth. Cryst.* **38** 870 (in Chinese)

[15] Lin Q G, Gao X Y, Liu Y F and Lu J X 2008 *Chin. J. Vacuum Sci. Technol.* **28** 566 (in Chinese)